

# Enhanced Short Time Peak in Four-point Dynamic Susceptibility in Dense Active Glass-forming Liquids

Subhodeep Dey,\* Anoop Mutneja,\* and Smarajit Karmakar†  
Tata Institute of Fundamental Research, 36/P, Gopanpally Village,  
Serilingampally Mandal, Ranga Reddy District, Hyderabad, 500046, Telangana, India

## I. MODELS AND METHODS

In this work, we have performed extensive molecular dynamics simulation of Binary mixture of Lennard-Jones (BMLJ) particles interacting via the following potential. The potential is smoothed such that  $2^{nd}$  derivative of the potential will be continuous at the cut off radius  $r_c$ ,

$$\phi(r) = \begin{cases} 4\epsilon_{\alpha\beta} \left[ \left( \frac{\sigma_{\alpha\beta}}{r} \right)^{12} - \left( \frac{\sigma_{\alpha\beta}}{r} \right)^6 + c_0 + c_2 r^2 \right] & , r < r_c \\ 0 & , r \geq r_c \end{cases} \quad (1)$$

Here,  $\alpha$  and  $\beta$  refers to large ( $A$ -type) or small ( $B$ -type) particles respectively. The ratio of  $A : B = 80 : 20$  is maintained. This model is well known in the literature as the Kob-Andersen model (3dKA) [1]. The interaction strengths and particle diameters are  $\epsilon_{AA} = 1.0$ ,  $\sigma_{AA} = 1.0$ ,  $\epsilon_{AB} = 1.5$ ,  $\sigma_{AB} = 0.8$ , and  $\epsilon_{BB} = 0.5$ ,  $\sigma_{BB} = 0.88$ , and  $r_c = 2.5\sigma_{AB}$ . The number density ( $\rho$ ) of the system is taken to be 1.2 for all the simulations. The units of length, energy and time are given by  $\sigma_{AA}$ ,  $\epsilon_{AA}$  and  $\sqrt{\frac{\sigma_{AA}^2}{\epsilon_{AA}}}$  respectively. The integration step size is chosen to be  $\delta t = 0.005$  for all our simulations.

### A. Introducing Activity: Run and Tumble particle model (RTP)

Activity in this study is introduced in the system by randomly choosing the  $c$  fraction of particles as active particles. The active particles get an extra active force  $f_0$  along any random direction while keeping zero vector sum of total active forces. The direction of the active force changes after the persistent time  $\tau_p$ . The active force on  $i^{th}$  particle reads as,

$$F_i^A = f_0 (k_x^i \hat{x} + k_y^i \hat{y} + k_z^i \hat{z}), \quad (2)$$

where  $k_x^i$ ,  $k_y^i$ ,  $k_z^i$  are randomly chosen from  $\pm 1$ , after every persistent time interval. Thus an active particle can have one of the eight possible directions. Also, to maintain the momentum conservation of the system, there should be an even number of active particles in the system with total active force equated to zero, which

mathematically implies,  $\sum_{\alpha,i} k_{\alpha}^i = 0$ . Thus, the total activity in our system is defined by three parameters, the active force magnitude  $f_0$ , the concentration of active particles  $c$ , and the persistent time  $\tau_p$ . In this study, we have first varied  $f_0$  in the range  $f_0 \in [0.0 - 2.5]$  while keeping  $c = 0.1$  and  $\tau_p = 1.0$  constant. Then the concentration  $c$  is varied in range  $c \in [0.0 - 0.6]$  while keeping  $f_0 = 1.0$  and  $\tau_p = 1.0$ . Note that we haven't changed the persistent time in this study. As large persistent time leads to a complete dynamical behaviour of the system as reported in [2], we kept it small and fixed to study the effect of activity in the glassy regime only.

## II. THERMOSTAT

The thermostat is one of the main challenges in non-equilibrium simulations. In particular, it seems that various thermostats fail to maintain a constant temperature in the presence of active forces. Thus, we have used the three-chain Nosé-Hoover thermostat [3] to get the desired temperature which is known to maintain true canonical ensemble fluctuations in equilibrium. The relaxation time of the thermostat is set to 10 – 20 times the simulation time-step. We also checked another thermostat known as Gaussian thermostat [4], which is also found to be able to control the temperature well in the presence of activity. The results obtained using these two thermostats are quantitatively similar.

## III. OVERLAP CORRELATION FUNCTION, $Q(t)$

To characterize the system's dynamical properties, we have computed the two-point density-density correlation function of the system. For simplicity, we have computed the overlap correlation function  $Q(t)$ , defined as

$$Q(t) = \frac{1}{N} \sum_{i=1}^N w(|\vec{r}_i(0) - \vec{r}_i(t)|), \quad (3)$$

where  $w(x)$  is a window function, and it is one if  $x < a$ , where  $a$  is a parameter that is chosen to remove the possible initial decorrelation that can happen due to the fast vibrational motion of the particles.  $\vec{r}_i(t)$  is the position vector of particle  $i$ . The value of 'a' is typically chosen from the plateau region in the system's 'mean-square

\* These authors contributed equally

† smarajit@tifrh.res.in

displacement (MSD)', where MSD is defined by the following expression.

$$\langle |\Delta r(t)|^2 \rangle = \left\langle \frac{1}{N} \sum_{i=1}^N |\vec{r}_i(t) - \vec{r}_i(0)|^2 \right\rangle \quad (4)$$

In the supercooled liquid regime, the MSD shows a plateau representing the cage exploration of the system during the transition of the particle dynamics from the ballistic to diffusion region. One often chooses this value to maximize the signal strength of the fluctuations of  $Q(t)$ , which is defined later as  $\chi_4(t)$ . We will discuss this in detail in the subsequent paragraph. Typically, the value of 'a' is chosen to be 0.3. This relaxation time,  $\tau_\alpha$ , is obtained as  $\langle Q(t = \tau_\alpha) \rangle = e^{-1}$  where  $\langle \dots \rangle$  refers to ensemble average. The system is equilibrated long enough (typically  $\sim 50\tau_\alpha$ ) so that the system's dynamic is ergodic in nature. We did further 4  $\tau_\alpha$  long runs for gathering data. We averaged our data over 32 statistically independent ensemble runs for all systems  $N \leq 10000$  and 10 simulations runs for  $N > 10000$  respectively.

#### IV. FOUR-POINT CORRELATION FUNCTION, $\chi_4(t)$

Four-point correlation susceptibility,  $\chi_4(t)$  is the measure of the fluctuation in two-point correlation function  $Q(t)$ . It is defined as

$$\chi_4(t) = N [\langle Q(t)^2 \rangle - \langle Q(t) \rangle^2]. \quad (5)$$

We averaged  $\chi_4(t)$  over 32 ensembles for simulations with  $N \leq 10000$  particles and 10 ensembles for  $N > 10000$ .

Note that  $\chi_4(t)$  is one of the best ways to characterize the degree of heterogeneity in a system. This typically quantifies the sizes of different regions with fast and slow dynamics. The time at which  $\chi_4(t)$  peaks is close to the relaxation time  $\tau_\alpha$  that is  $\chi_4(t = \tau_\alpha) \simeq \chi_4^p$ . The increasing system size shows one more peak at shorter timescale around the  $\beta$ -relaxation regime. It is found that peak at short timescale can be enhanced by a suitable choice of the cut-off parameter 'a'. For  $a = 0.3$ , most of the small-amplitude motion of the particle is masked, which is important to pick up the long-wavelength mode at low temperatures. To enhanced the peak height of  $\chi_4(t)$  at short timescale we have chosen  $a = 0.18$ . The peak at short timescale is defined as  $\chi_4^{P1}$  and the time corresponding to the first peak (maxima) of  $\chi_4(t)$  as  $t^*$ .

#### V. $\beta$ -RELAXATION TIME ( $\tau_\beta$ )

The  $\beta$ -relaxation time scale  $\tau_\beta$ , is defined as the time when a point of inflection appears in the log-log plot of MSD with respect to time [5]. Thus it is usually calculated as the time where the minima of log-derivative of MSD with time,  $d \log \langle |\Delta r(t)|^2 \rangle / d \log t$  appears.

## VI. CAGE-RELATIVE DISPLACEMENT

To separate out the collective behaviour that may arise from the vibrational dynamics, especially at a short timescale, we have computed the cage-relative (CR) displacement of the individual particles, which is defined as  $\vec{r}_{i,CR}(t)$ .

$$\vec{r}_{i,CR}(t) = [\vec{r}_i(t) - (\vec{r}_{i,nn}(t) - \vec{r}_{i,nn}(0))] \quad (6)$$

where,  $\vec{r}_{i,nn}(t)$  is center of mass position of  $N_{nn}$  nearest neighbours (nn) at time  $t$  and it is defined as,

$$\vec{r}_{i,nn}(t) = \frac{1}{N_{nn}} \sum_{j=1}^{N_{nn}} [\vec{r}_j(t) - \vec{r}_j(0)]. \quad (7)$$

Here we have used the cut-off value  $r_c^{nn} = 1.3$  at the initial time to get the  $N_{nn}$  number of nearest neighbours and then track those neighbour particle's motion with respect to that time origin. This modified cage- relative displacement quantity has then been used to compute both cage-relative  $Q(t)$  and  $\chi_4(t)$ .

## VII. BLOCK ANALYSIS

In this work, we have done extensive finite-size scaling analysis using the Block analysis method [6]. In this method, the whole system is divided into smaller subsystems, and then one studies all the above-mentioned correlation functions to incorporate some of the important fluctuations. For example,  $\chi_4(t)$  will have contributions coming from a number of particle fluctuations, density fluctuations, the concentration of particle species fluctuations, temperature fluctuations, etc. This is also one of the most natural ensembles, especially in experiments in which a subsystem is typically probed using various imaging methods. The two-point correlation for one subsystem can be redefined similarly as,

$$Q(L_B, t) = \frac{1}{n_i} \sum_{j=1}^{n_i} [w(r_j(t) - r_j(0))], \quad (8)$$

where  $L_B = (N/N_B)^{1/3}$  and,  $N_B$  is the number of subsystems referred henceforth as blocks.  $n_i$  is the number of particles in the block with level  $i$ . Now the average correlation of the function will be just

$$\langle Q(L_B, t) \rangle = \frac{1}{N_B} \sum_{i=1}^{N_B} Q(L_B, t). \quad (9)$$

Similarly, the four-point susceptibility per particle for each block can be written as

$$\chi_4'(L_B, t) = [\langle Q(L_B, t)^2 \rangle - \langle Q(L_B, t) \rangle^2]. \quad (10)$$

So the averaged four-point dynamic susceptibility of the sub-system ( $L_B$ ) will be given by

$$\chi_4(L_B, t) = \left( \frac{N}{N_B} \right) [\chi_4'(L_B, t)]. \quad (11)$$

In this case  $\langle \dots \rangle$  denotes averages over different grand canonical ensembles of size  $L_B$ .

### VIII. CHOICE OF TEMPERATURE FOR DIFFERENT ACTIVITY

To compare the effect of different activity we have fixed the relaxation time  $\tau_\alpha$  for all the systems. For which we have looked at the temperature dependence of  $\tau_\alpha$  for different value of activity parameter  $\Omega = cf_0^2\tau_p$ . Here  $c$  is the concentration of the active particles,  $f_0$  is the magnitude of the applied active force, and  $\tau_p$  is the persistent time over which the directions of active forces change randomly. The change of  $\tau_\alpha$  for different  $T$  can be fitted well via VFT (Vogel-Fulcher-Tammann) fitting function (see top panels of Fig.1)

$$\tau_\alpha = \tau_0 \exp[A/(T - T_0)]. \quad (12)$$

By using the above fitting equation, we can find the temperature corresponding to a fixed relaxation time  $\tau_\alpha$  for a different activity. Here we have fixed the relaxation time  $\tau_\alpha$  corresponding to  $T = 0.45$  of a passive system, which is around  $\tau_\alpha \sim 2200$  for  $N = 1000$  particles. Firstly, the changes because of  $f_0 = 0.0, 0.5, 1.0, 1.5, 2.0, 2.5$  has been studied for  $c = 0.1$ , and,  $\tau_p = 1.0$ , as shown in top left panel of Fig.1 and then the changes because of  $c = 0.0, 0.1, 0.2, 0.3, 0.4, 0.5, 0.6$  are studied for fixed  $f_0 = 1.0$ , and,  $\tau_p = 1.0$  as shown in the top right panel of Fig.1. Subsequently, we choose the temperatures so that the relaxation time is the same across various activities for  $N = 1000$ . The corresponding correlation functions for these temperatures are shown in the bottom panels of Fig.1. One can see that the two-point correlation function falls on top of each other. The value of  $a$  is 0.3 in this case.

### IX. FIRST PEAK OF DYNAMIC SUSCEPTIBILITY

As discussed in the main article, we set the value of  $a = 0.18$  while studying  $\chi_4(t)$  especially at short timescale. This allowed us to pick the first maximum of dynamic heterogeneity curve in the early-beta region very effectively.

As reported in Ref.[7], the degree of activity in the system can be quantified using a unique parameter  $\Omega = cf_0^2\tau_p$  and as long as  $\Omega$  is same with various possible combinations of  $c$ ,  $f_0$  and  $\tau_p$ , the dynamical behaviour should

be same. This is also known to be true over a small window of parameter values. In this study, we found that over the studied range of parameter values, this unique activity parameter,  $\Omega$  faithfully captures the effective degree of activity in the system. The system size dependence of  $\chi_4^{P1}$  for canonical ensemble is very different from that of grand canonical ensemble as discussed before. In the main article we have presented the data pertaining to the subsystems where all possible fluctuations can be included while measuring  $\chi_4(t)$ . The system size dependence of  $\chi_4^{P1}$  when calculated for the full system is presented in Fig.3(a) for reference. Note that dependence is very similar to that of the subsystems (blocks) and overall conclusions do not change qualitatively even if one works with  $\chi_4^{P1}$  for the full systems but there are some issues that we observed while working with full system size data. Some of these are elaborated in the subsequent sections.

### X. SCALING ANALYSIS OF $\chi_4^{P1}$ USING FULL SYSTEM

In the main text, we presented the finite-size data of  $\chi_4^{P1}$ , calculated for the quarter of the system length, i.e.,  $L/4$ . Here in Fig.3, we present the full system size data and the best scaling collapse possible by using the length scale obtained from  $g^{uu}(r, t^*)$ . One can see that the larger system size and larger activity data points are coming out of the collapse, which we infer are coming because of the missing fluctuations in the system as well as averaging issues, as mentioned in the main text. Once we take quarter of the systems for the doing the analysis (as shown in the main article) the issues disappear which can be due to two reasons. First being that with quarter system size, one will have much better averaging as well as it is going to include all possible missing fluctuations that are important in  $\chi_4(t)$ . The second reasons can be that the system size itself became smaller and if one does simulations of much bigger system sizes then one will again see the same deviation. At this moment we are constrained by the larger system size ( $N = 100000$ ) in our hand due to computational expense, so ruling out the second possibility is not possible at this moment. The important part of this analysis is that the scaling ansatz still seems to be quite good to describe most part of the data.

### XI. DISPLACEMENT-DISPLACEMENT CORRELATION FUNCTION, $g^{uu}(r, t)$

The dynamical length scale of the system  $\xi_d$  can be computed independently by computing the displacement-displacement correlation function  $g^{uu}(r, t^*)$  at  $t^*$  [8, 9].

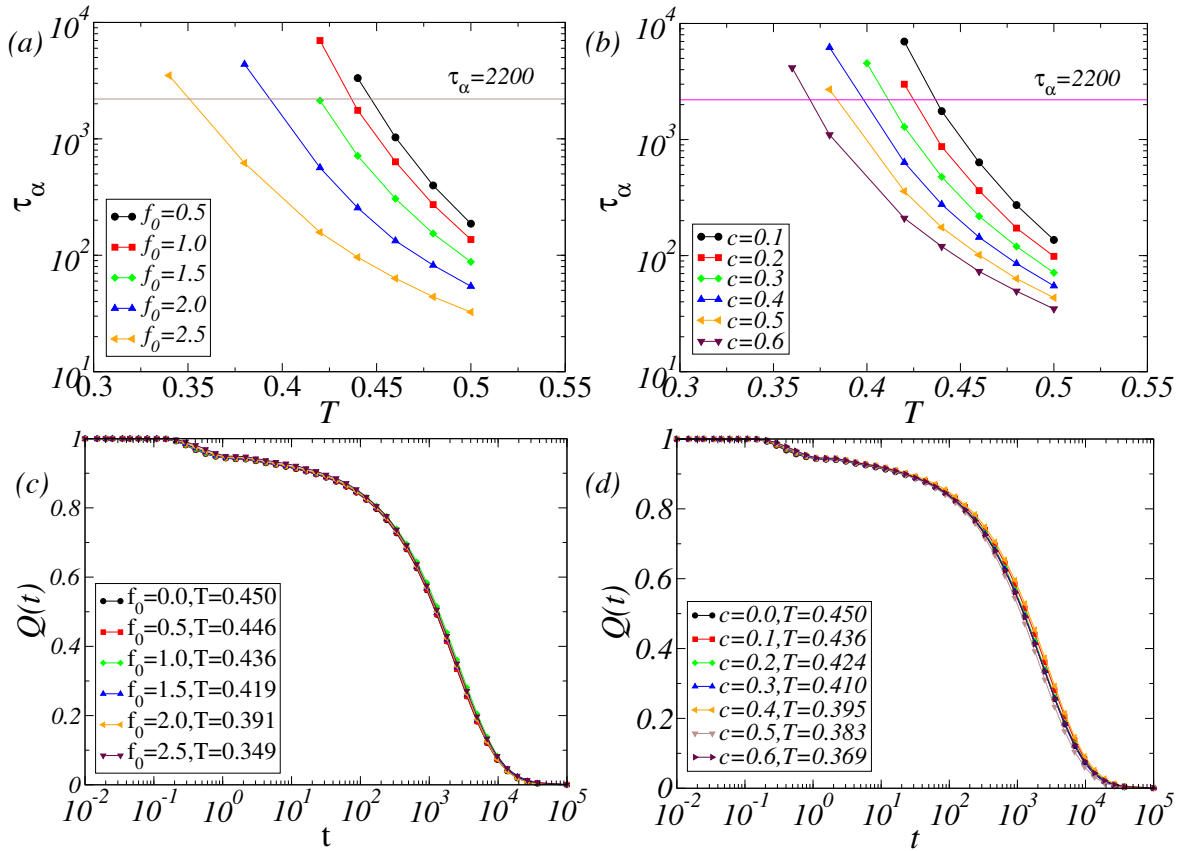


FIG. 1. (a). Relaxation time  $\tau_\alpha$  vs temperature  $T$  for different driving  $f_0$  with fixed concentration of active particles  $c = 0.1$  and persistent time  $\tau_p = 1.0$ . Here the system size  $N = 1000$ . (b). Similar results for varying concentration at fixed value of  $f_0 = 1.0$  and  $\tau_p = 1.0$ . (c). Two-point correlation function  $Q(t)$  vs time  $t$ . Here the temperature is chosen such that the relaxation time ( $\tau_\alpha$ ) for different activity ( $f_0$ ) is around 2200. (d). Similar plots when we varied the concentration of active particles  $c$  keeping  $f_0 = 1.0$  and  $\tau_p$  constant.

It is defined as,

$$g^{uu}(r, \Delta t) = \frac{\left\langle \sum_{i,j=1, j \neq i}^N u_i(0, \Delta t) u_j(0, \Delta t) \delta(r - |\mathbf{r}_{ij}(0)|) \right\rangle}{4\pi r^2 \Delta r N \rho \langle u(\Delta t) \rangle^2} \quad (13)$$

where,  $u_i(t, \Delta t) = |\mathbf{r}_i(t + \Delta t) - \mathbf{r}_i(t)|$ , and  $\langle u(\Delta t) \rangle = \langle \frac{1}{N} \sum_{i=1}^N u_i(t, \Delta t) \rangle$ .  $g^{uu}(r, \Delta t)$  is calculated at time  $\Delta t = t^*$ , along with the usual pair correlation function  $g^r(r)$  defined as,

$$g^r(r) = \frac{\left\langle \sum_{i,j=1, j \neq i}^N \delta(r - |\mathbf{r}_{ij}(0)|) \right\rangle}{4\pi r^2 \Delta r N \rho} \quad (14)$$

For far enough particles the displacement over a large enough time duration would be decorrelated and  $g^{uu}$  would be equal to  $g^r$ . So the quantity  $g^{uu}(r, \Delta t)/g^r - 1.0$  would decay to zero as a function of  $r$ . Fit of peak heights to a function  $f(r) = A \exp(-r/\xi)/r^\alpha$  should give us a length scale. But the area under the curve would provide us better way to obtain the same correlation length. Fig.4(a) contains the plot of  $\log(g^{uu}(r, \Delta t)/g^r - 1.0)$  calculated for system size of  $N = 10^5$ . The obtained length scale ( $\xi_{uu}$ ) via fitting and integrated area is plotted in Fig.4(b) for different activity in the system.

[1] W. Kob and H. C. Andersen, Phys. Rev. E **51**, 4626 (1995).

[2] R. Mandal, P. J. Bhuyan, P. Chaudhuri, C. Dasgupta, and

M. Rao, Nat. Comm. **11**, 2581 (2020).

[3] M. P. Allen and D. J. Tildesley, *Computer Simulation of Liquids* (Clarendon Press, New York, NY, USA, 1989).

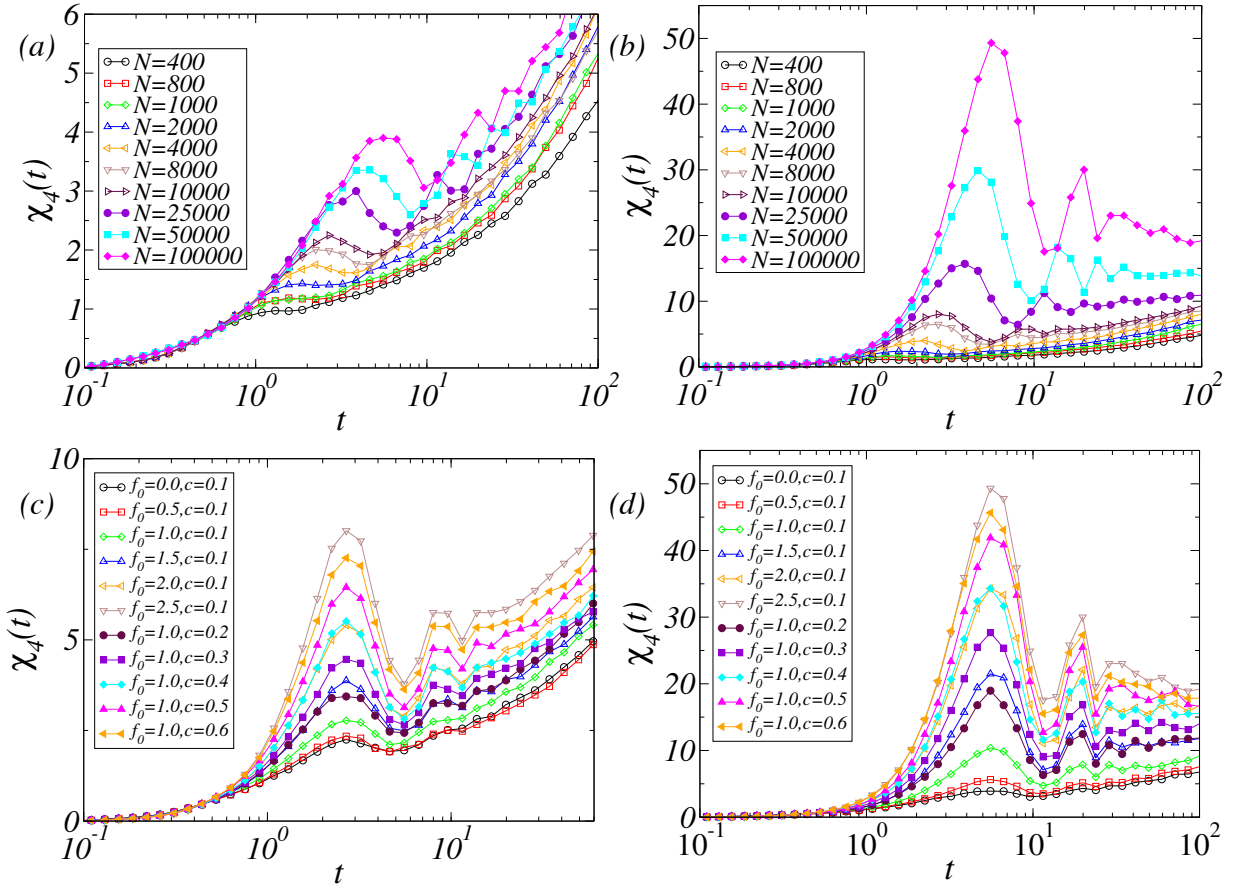


FIG. 2. (a). Dynamic susceptibility  $\chi_4$  vs time  $t$ , for a passive 3dKALJ model at temperature  $T = 0.45$  for various system sizes in the range  $N \in [400 - 100000]$ . One can clearly see the huge increase in peak height with increasing system size. Note that the time at which  $\chi_4(t)$  peaks also increases with the system size. (b). Similar plot for active system with  $f_0 = 2.5$  at temperature where  $\tau_\alpha \sim 2200$  similar to the passive case. Notice the dramatic enhancement (nearly 10 fold) of the peak with increasing activity. (c,d) Variation of  $\chi_4(t)$  peak with changing activity for  $N = 10000$  (left) and  $N = 100000$  (right) particle system.

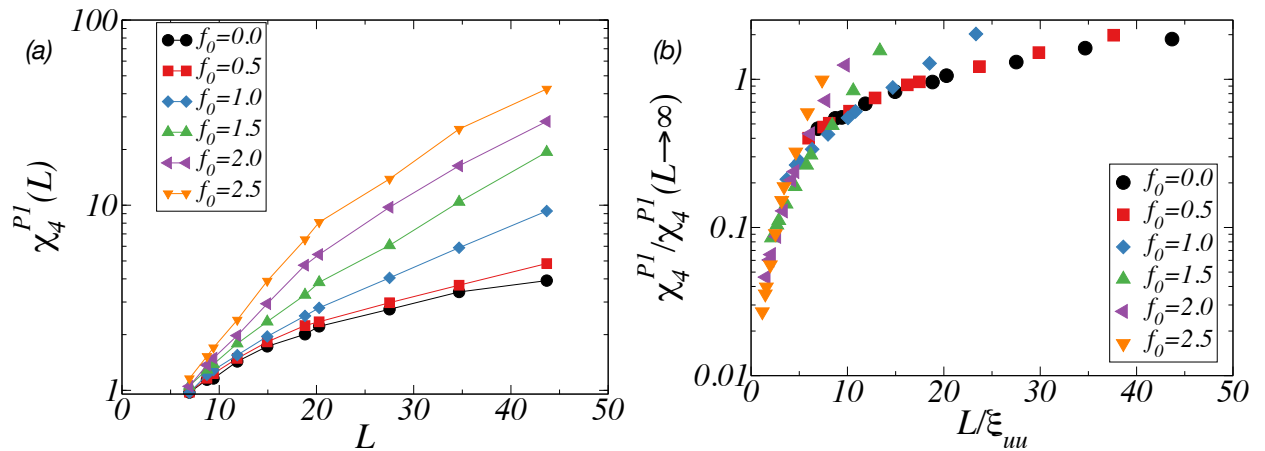


FIG. 3. (a) The system size dependence of  $\chi_4^{P1}$  is plotted for systems with different active forces  $f_0$  and the same concentration of active particles,  $c = 0.1$ . (b) The finite system size data is tried to collapse using the length scale obtained from the displacement-displacement correlation function ( $\xi_{uu}$ ). The data collapse obtained is not that great as presented for  $L/4$  system size but does not dismiss the presence of the scaling ansatz.

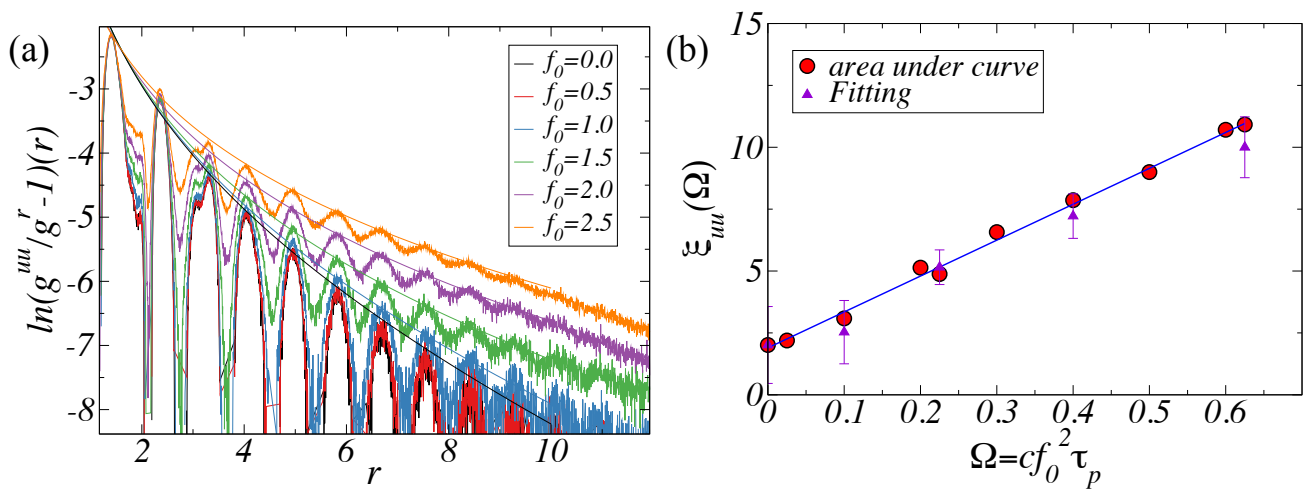


FIG. 4. (a) The quantity  $\log(g^{uu} - g^r)/g^r(r, \Delta t)$  is plotted as a function of spatial distance for  $\Delta t = t^*$ , here  $g^{uu}(r, \Delta t)$  is the displacement-displacement correlation function (Eq.13), and  $g^r$  is the pair correlation function. Lines in the plots are fit of peak heights to a function  $f(x) = a - x/\xi - \alpha \log(x)$ , to obtain the length scale  $\xi$ . The obtained length scale can be clearly seen increasing with increasing activity. This non-linear three parameter fit is not a good idea, because of the errors involved. The length scale variation with increasing activity can also be obtained as an integrated area of the plots and is shown in panel (b).

[4] F. Zhang, J. Chem. Phys. **106**, 6102 (1997).

[5] S. Karmakar, C. Dasgupta, and S. Sastry, Phys. Rev. Lett. **116**, 085701 (2016).

[6] S. Chakrabarty, I. Tah, S. Karmakar, and C. Dasgupta, Phys. Rev. Lett. **119**, 205502 (2017).

[7] R. Mandal, P. J. Bhuyan, M. Rao, and C. Dasgupta, Soft

Matter **12**, 6268 (2016).

[8] I. Tah and S. Karmakar, Phys. Rev. Research **2**, 022067 (2020).

[9] P. H. Poole, C. Donati, and S. C. Glotzer, Physica A: Statistical Mechanics and its Applications **261**, 51 (1998).